American Journal of Traffic and Transportation Engineering
2024, Vol. 09, No. 3, pp. 41-53
https://doi.org/10.11648/j.ajtte.20240903.11

Research Article

Simulation of Ship Berthing Operation at Luojing Container Terminal Under Extreme Sea Conditions

Haidong Zhan[1], Feng Zhu[1], Jianwen Wu[1], Jie Wang[2, *]

[1]Shanghai Maritime Pilots' Association, Shanghai, China

[2]Merchant Marine College, Shanghai Maritime University, Shanghai, China

Abstract

The Luojing Port Area of the Port of Shanghai, specifically the coal terminal and ore terminal, used to be the main port area for coal and ore bulk cargo transportation services in the Port of Shanghai.To enhance the container handling capacity at Shanghai port, this study conducted a series of simulation tests at Luojing Container Terminal. The tests were designed according to the terminal's specifications, taking into account the limit berthing wind direction and wind speed (levels 6 and 7). This study selected an appropriate representative ship type for the comprehensive simulation tests, and it thoroughly tested the berthing limits under various extreme conditions using an advanced navigation simulator. The experiment obtained the motion parameters and trajectory of the simulated ship. Based on these results, this study analyzed and evaluated the safety of the rotary waters and berthing operations, ensuring they met the safety assessment requirements for wharf engineering. The study examined the berthing time window, berthing mode, boundary conditions, and safety guarantee measures under extreme sea conditions at Luojing Container Terminal. Finally, By analyzing the berthing simulation trajectory diagrams, tugboat usage, and vessel maneuvering data under the eight extreme berthing conditions, this study formulated a safe berthing plan for ships.

Keywords

Extreme Sea Conditions, Luojing Port Area, Navigation Simulator, Unberthing Operation, Simulation Test

1. Introduction

Luojing Port Coal Terminal and Ore Wharf of Shanghai Port have been primary ports for coal and ore bulk cargo transportation. Relying on the location advantage and the Yangtze estuary's 12.5-meter deepwater channel regulation advantage, they have become key points for foreign trade ore shipments into the Yangtze River Delta. They serve as transit hubs for importing iron ore for steel mills along the Yangtze River, providing an optimal comprehensive cost solution.

According to the central ecological and environmental protection supervision, key verification results of the Yangtze River trunk line utilization project, and the Shanghai Three-year Action Plan for Environmental Protection and Construction 2018-2020, Luojing Coal Terminal and Luojing Ore Terminal were suspended in 2018 and 2019 respectively, and the terminals are currently idle. To continuously improve the container handling capacity of Shanghai Port, it is urgent to enhance the level of the Shanghai International Shipping Center and increase the shoreline resources of container terminals. Therefore, it is necessary to carry out simulation tests of ship operations under extreme sea conditions to provide

*Corresponding author: wangjie1@shmtu.edu.cn (Jie Wang)

Received: 1 July 2024; **Accepted:** 23 July 2024; **Published:** 6 August 2024

technical support and ensure the berthing safety of the ships and the navigation safety of the related waters.

Shanghai Port is located in a subtropical monsoon climate zone and is influenced by the East Asian monsoon. Due to the effects of the marine climate, as well as the continental and marine monsoons in winter and summer, the region experiences alternating cold and warm air masses, leading to complex weather changes. Shanghai Port experiences four distinct seasons with a mild and humid climate, abundant rainfall, sufficient sunlight, and a long frost-free period. Spring and autumn are shorter, while winter and summer are longer. Spring is warm and cool with frequent continuous rain, and some years may experience cold spells. Summer is hot and humid, often bringing drought, waterlogging, typhoons, hail, and other severe weather conditions, resulting in extreme sea conditions. Extreme sea conditions refer to the state of the sea surface caused by wind, waves, and surges, as well as the physical, chemical, and biological properties observed in marine hydrology. Under extreme sea conditions, the stability of ships can be compromised due to the forces of wind, currents, and waves, increasing the difficulty of ship operations and the risk of collisions.

Zhang Yecheng [1], based on the MMG (Mathematical Maneuvering Group) model, obtained the four degrees of hydrodynamic derivatives of freedom to forecast the rotational movement and Z-shaped maneuvering movement. Wu Rocinante [2] designed a ship restraint model test platform based on the Stewart six-degrees-of-freedom parallel mechanism. Yi Qun [3] adopted the method of model testing to study the motion characteristics of a cylindrical floating production, storage, and offloading device under different laboratory-simulated ocean currents. Vanem Erik [4] analyzed the effective wave height dataset provided in the second environmental extreme benchmark test submitted in OMAE 2021. Li Mingxin [5] established a multi-ship hydrodynamic numerical model under wave impact based on the time domain Rankine source surface method to study the hydrodynamic performance and motion characteristics of ships when advancing in waves. Yan Mingyu [6] used the mixed Boussinesq-park 1 model to simulate the hydrodynamic response of moored container ships caused by irregular waves. Van Zwijnsvoorde Thibaut [7] introduced a practical model predictive controller for path tracking of surface ships and tested it experimentally. Guo Bingjie and Gupta Prateek [8] proposed two different methods to estimate VTI (Vertical Transverse Isotropy), verifying their applicability and comparing their performance. Rueda Bayona Juan Gabriel [9] proposed an alternative experimental and analytical method to measure the near-field flow-solid coupling under wet conditions and quantify the measured structure and 3D hydrodynamic acceleration. Liu Guilin [10] proposed a nested random composite distribution (NSCD) model based on the stochastic process theory. Huang Ming [11] studied the adverse condition factors and key operations affecting the unberthing of LNG (Liquefied Natural Gas) ships in bad weather. Meng Yao [12] pointed out that the premise of ship operational forecast is to establish an accurate mathematical model of ship movement. Bian Hongwei [13] designed a new ship motion parameter generator based on the mobility characteristics of the ship itself, capable of generating various ship motion parameters required by the navigation simulator. Zhang Yue [14] established a mathematical model of the interference force and torque of wind and flow, analyzing the operational efficiency of the side thrust device to assist ship movement under different working conditions. Jing Qianfeng and Sasa Kenji [15] found that significant wave height, wind speed, mean wave period, ocean current velocity, wind apparent direction, and wave encounter angle are the most statistically significant factors for rudder attenuation.

The literature reviews the research on ship motion and hydrodynamic performance from different angles. It covers ship maneuvering, model predictive controllers, and fluid-structure interaction. The aim is to improve ship maneuvering performance and safety. This research is particularly significant for ship berthing at the Luojing container terminal in extreme sea conditions.

2. Establishment of the Mathematical Model of Ship Movement

2.1. Coordinate System Selection

The mathematical model of ship motion uses two coordinate systems as shown in Figure 1: one is a space-fixed coordinate system $O_0X_0Y_0Z_0$, where the origin O_0 can be chosen arbitrarily, the O_0X_0 points to the north, the O_0Y_0 points to the east, and the O_0Z_0 is vertically downward as positive, with the $X_0O_0Y_0$ plane located at the still water surface; the other is a ship-moving coordinate system G_{xyz}, where the origin G is the ship's center of gravity, the G_x points to the bow, the G_y points to the starboard, and the G_z points vertically downward to the keel. Usually, the origin of the coordinate system is chosen to be consistent with the position of G.

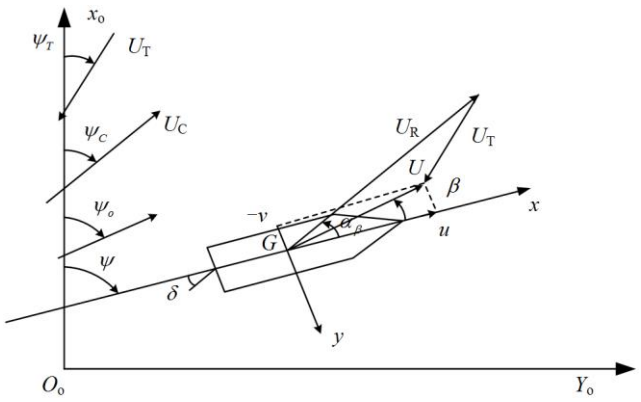

Figure 1. *Ship motion coordinate system.*

In Figure 1, ψ represents the heading angle; U is the resultant speed of the ship's motion, U_T and U_R are the absolute and relative wind speeds; ψ_T and α_R are the absolute and relative wind angles; U_C and ψ_C are the current speed and current direction angle; ψ_W is the absolute wave direction angle; β is the drift angle; δ is the rudder angle, with the right rudder being positive. Below, the mathematical model of ship motion will be established in the two coordinate systems shown in Figure 1.

2.2. Equation of Four Degrees of Freedom

The mathematical models for the four degrees of freedom in the maneuvering motion—surge, sway, yaw, and roll—are as follows:

$$(m+m_x)\dot{u}-(m+m_y)vr = X_H + X_p + X_R + X_A + X_{w1} + X_{w2} + X_B + X_L + X_T + X_C + \cdots \quad (1)$$

$$(m+m_y)\dot{v}+(m+m_x)ur = Y_H + Y_P + Y_R + Y_A + Y_{W1} + Y_{W2} + Y_B + Y_L + Y_T + Y_C + \cdots \quad (2)$$

$$(I_{zz}+J_{zz})\dot{r} = N_H + N_p + N_R + N_A + N_{W1} + Y_{W2} + N_B + N_L + N_T + N_C + \cdots \quad (3)$$

$$(I_{xx}+J_{xx})\dot{p} = K_H + K_R + K_A + K_{W1} + Y_{W2} + K_B + K_L + K_T + K_C + \cdots \quad (4)$$

In the formula, X, Y, N and K are the external forces and moments acting on the ship's hull; u, v, r and p are the components of the ship's motion in the horizontal plane, the yaw rate, and the roll rate; m is the mass of the ship; $m_x$and$m_y$are the added masses in the x and y directions, respectively;$I_{xx}$and$I_{zz}$are the moments of inertia about the x and z axes, respectively; J_{xx} and J_{zz} are the added moments of inertia about the x and z axes, respectively. The subscripts on the right-hand side of the equations have the following meanings: H for the bare hull; P for the propeller; R for the rudder; A for the wind; $W1$ and $W2$ for the first and second-order wave forces; S for the shore; L for the mooring lines; T for the tugboat; C for the external forces and moments generated by the anchor chain acting on the ship's hull.

2.3. Calculation Model of Wind Disturbance Force

When a ship is navigating at sea or in a port, its superstructures will be affected by wind forces, causing the ship to deviate from its course or making maneuvering difficult. The impact of wind on ship maneuverability is particularly significant when navigating at low speeds in a port. In the wind force calculation model, the actual wind speed and direction are referred to as the absolute wind speed and direction, while the wind speed and direction perceived on the ship are referred to as the relative wind speed and direction.

Absolute or true wind is a wind observed in the inertial frame fixed to Earth, with absolute wind speed shown as U_T and absolute wind direction by wind angle ψ_T. The ψ_T of north wind is 0 and the ψ_T of east wind is 90, and the change of ψ_T ranges from 0 to 360. In fact, the wind pressure and torque of the ship are directly related to the relative wind speed or visual wind. The relative wind speed is the wind observed in the attachment coordinate system. The relative wind speed U_R and the relative wind direction angle α_R are the wind speed and wind direction value measured by the anemometer on the ship. Provide $\alpha_R < 0$ for wind from starboard and $\alpha_R > 0$ from starboard. The absolute wind speed U_T is the sum of the vector between the ship speed U and the relative wind speed U_R.

$$U_R = U_T - U \quad (5)$$

By projecting the above equations onto the axes of the two body-fixed coordinate systems, we obtain:

$$u_R = u + U_T cos(\psi_T - \psi) \quad (6)$$

$$v_R = -v + U_T \sin(\psi_T - \psi) \quad (7)$$

Where U_T is the value of absolute wind speed; two components of U_R. The wind angle is calculated as follows:

$$\alpha_R = \arctan\frac{v_R}{u_R} + \alpha c \quad (8)$$

$$\alpha c = \begin{cases} -\pi sgn(v_R) \\ 0\ (u_R < 0) \end{cases} (u_R \geq 0) \quad (9)$$

The average wind pressure and moment acting on the hull are:

$$X_A = \frac{1}{2}\rho_A A_f U_R^2 C_{Xa}(\alpha_R) \quad (10)$$

$$Y_A = \frac{1}{2}\rho_A A_s U_R^2 C_{Ya}(\alpha_R) \quad (11)$$

$$N_A = \frac{1}{2}\rho_A A_s L_{oa} U_R^2 C_{Na}(\alpha_R) \quad (12)$$

Where, ρ_A is the air density; A_f is the positive projection area of the building on the waterline on the hull; A_s is the projection area on the hull on the waterline; L_{oa} is the total length of the ship; $C_{Xa}(\alpha_R)$, $C_{Ya}(\alpha_R)$,$C_{Na}(\alpha_R)$ is the wind pressure coefficient, which is generally obtained by the wind tunnel test and can be calculated by the regression formula.

2.4. Dynamic Calculation Model of the Flow

In this model, the flow is treated as quasi-uniform flow. The navigation area is divided into segments, and each segment is

treated as uniform flow. The forces exerted by the uniform flow on the hull are incorporated into the hydrodynamic calculations using the relative velocity method, and the additional forces generated by the presence of the flow are also considered. Assuming the flow is constant and uniform, it only changes the position and speed of the ship without altering its heading. Thus, the disturbance force model of the ocean current can be expressed as:

$$X_{curent} = mU_C\cos(\varphi c - \psi - \pi) \quad (13)$$

$$Y_{curent} = mU_C\sin(\varphi c - \psi - \pi) \quad (14)$$

$$N_{current} = 0 \quad (15)$$

2.5. 10,000-ton Container Ship Test Ship Type

The 10,000-ton container ship is selected as the test object, and the test ship type, main parameters and basic ship type test data are as follows:

1) Test vessel type and main parameters

Table 1. *Test the ship type and main parameters.*

cabinet minister	148.0 m
ship beam	27.0 m
load draught	8.0 m
Host power	40000 HP
moulded depth	13.6 m

2) Basic ship type test

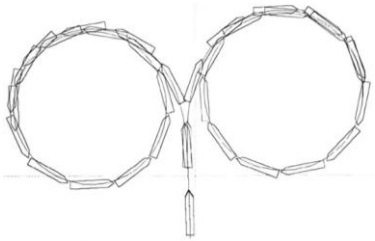

Figure 2. *Track diagram of left and right swing test of test ship type with full speed.*

Table 2. *Performance of left and right loop at full speed.*

Initial speed RPM and payload status	ship type	time (s)	error	feed pitch (m)	error	departure (m)	error
Full load at full speed Turn right first 90	The original ship type						
	Simulation ship	108		541		271	
Full load at full speed Turn right first 180	The original ship type						
	Simulation ship	185		292		553	
Full load at full speed Turn left first 90	The original ship type						
	Simulation ship	97		488		326	
Full load at full speed Turn left first 180	The original ship type						
	Simulation ship	174		256		606	

Table 3. *Test ship stroke.*

ship type	Load state	Initial speed	distance (m)	error	time (s)	error
Prototype ship	fully loaded	full speed				
Simulation ship			2176			

Table 4. Corresponding ship speed table of the test vessel speed.

carriage clock	Test ship type data		carriage clock	Test ship type data	
	Rpm	Speed (kn)		Rpm	Speed (kn)
DS-AHD	30	5.0	DS-AST	30	4.1
S-AHD	50	7.8	S-AST	50	6.3
H-AHD	70	10.7	F-AST	65	7.8
F-AHD	95	14.3	H-AST	80	9.5
SEASPD	110	16.5			

3. Ship Operation Simulation Test Preparation

3.1. Simulation and Test Equipment

The ship simulation maneuvering test used the large-scale navigation simulator of Shanghai Maritime University. The details of the navigation simulator are as follows:

1) Origin, model, category, price, introduction time, and viewing angle (degrees), etc.

The navigation simulator is independently developed by the university. The university has a research team dedicated to the long-term development of the simulator, providing navigation simulators for most maritime academies and training institutions in China.

The construction of the university's simulators has been carried out in multiple phases, with the first phase completed in 2007 and the most recent phase in 2014. The university possesses a sufficient number of simulators, covering a wide range of types, all certified by DNV, including one 360-degree large-scale navigation simulator with A-level qualification, two 120-degree navigation simulators with B-level qualification, one 180-degree navigation simulator, eight 120-degree LCD screen navigation simulators, and special simulators for yachts and offshore vessels, each with one unit. In total, there are 14 various types of navigation simulators. The laboratory housing these simulators is a national-level virtual teaching experimental center and the Ministry of Education's engineering center for maritime simulation.

2) Features of the simulator

The 360-degree navigation simulator independently developed by the university is currently the world's largest comprehensive research platform for maritime simulation systems. It meets the requirements of the STCW Convention for assessing the competency levels of seafarers using simulators and has passed the ISO9001 quality system audits by DNV and the China Maritime Safety Administration.

The navigation simulator creates a "large navigation" scenario composed of a "main vessel" and several "secondary vessels." Using a six-degrees-of-freedom ship motion mathematical model, it calculates the motion parameters of the "main vessel" based on the navigation environment and operational commands, generating a 360-degree multi-channel cylindrical screen projection. It can simulate the environments of more than 30 major ports worldwide.

The 3D visual scene of the university's simulator already covers the main domestic waterways and ports, with most of the Yangtze River waterways included and available as needed. It can simulate weather conditions such as day and night, rain and snow, wind and waves, fog, etc. It can realistically display various virtual environments of real ports under extreme sea conditions, as shown in Figure 3.

Figure 3. Comprehensive Ship Maneuvering Simulator Based on a 360-Degree Panoramic Stereoscopic Visual System.

3.2. Test Range

The width of the berthing waters in front of the outer dock at Luojing operational area is 91.5 meters, with a natural water depth between 12 to 14 meters (relative to the National 85 Datum, the same below). The near-term design depth is -15.46

meters (assuming ships are lightened to a draft of 13.2 meters), and the long-term design depth is -16.76 meters. The distance from the dock front to the northern boundary of the Baoshan South Channel is approximately 650 meters. The turning basin is arranged in front of the dock (as shown by the large ellipse in Figure 4), with the turning circle arranged in an elliptical shape. The major axis along the water flow direction is 2.5 times the ship length, or 865 meters, and the minor axis perpendicular to the water flow direction is 1.6 times the ship length, or 554 meters. The design depth is -12.5 meters (assuming ships are lightened to a draft of 13.2 meters).

The width of the berthing waters in front of the outer dock's back side berth is 46 meters, with a natural water depth between 6 to 8 meters, and the design depth is -10.56 meters. The distance between the large and small docks is approximately 400 meters. The turning basin turning circle is arranged in an elliptical shape (as shown by the small ellipse in Figure 4). The major axis along the water flow direction is 2.5 times the ship length, or 353 meters, and the minor axis perpendicular to the water flow direction is 2 times the ship length, or 282 meters. The natural water depth in front of the inner dock's inner front is between 3 to 6 meters, as shown in Figure 4.

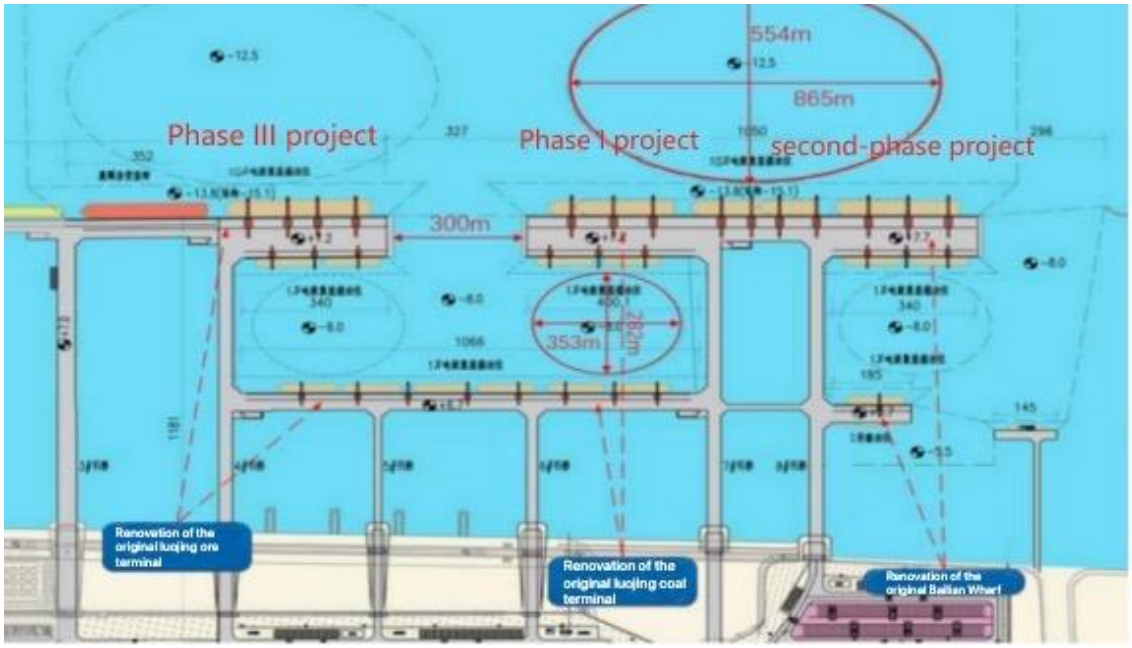

Figure 4. *General layout of container renovation and rotary waters of Luojing Port Area of Shanghai Port.*

3.3. Simulation Test Protocol

The ship motion mathematical models for the hull, wind, and current were integrated into the navigation simulator. A 10,000-ton container ship was used as the test vessel to analyze the operations at Luojing Container Terminal under extreme sea conditions.

According to meteorological statistics from the Baoshan meteorological station over the past three years (2020-2022), the prevailing wind directions are ESE and NNE, with maximum wind speeds reaching 23.1 m/s, mostly from the NE and ENE directions, and an average wind speed of 4.7 m/s. Considering the actual conditions at Shanghai Port, due to the influence of Jiang-Huai cyclones and Siberian cold air, ships in the Luojing operational area are affected by southeasterly winds of force 6 or higher during port entry and berthing operations. Given the orientation of the terminal, crosswind has a significant impact on berthing operations.

Additionally, based on the statistical analysis of short-term wave observation data over two years at Shidongkou (the prevailing wave direction in the nearby waters is ESE with a frequency of 21.68%, and the prevailing wave direction in Shanghai coastal and Yangtze estuary areas is quite consistent with the prevailing wind direction) ("Evaluation Report on Navigational Conditions for the Phase I Project of Luojing Container Terminal Reconstruction at Shanghai Port"), and fully considering the wind resistance level of ships in the inner harbor basin and the risks during entry and exit, the wind direction for berthing under extreme sea conditions in the simulation test was set to NE, with wind forces of 6 and 7.

Based on the analysis of environmental parameters for the test conditions, a combination of extreme berthing simulation test conditions was formulated. Each condition was tested 10 times to ensure the accuracy of the test data. The maneuvering conditions are shown in Table 5:

Table 5. 10,000 ton container ships (Phase I small wharf berth).

number	status	wind		flow		remarks
		wind direction	wind scale	Strength (kn)	flow direction (°)	
33	berth alongside	NE	6	3	125	Entry door
34	berth alongside	NE	6	3	125	Entry door
35	berth alongside	NE	7	3	125	Entry door
36	berth alongside	NE	7	3	125	Entry door
37	berth alongside	NE	6	2	305	Entry door
38	berth alongside	NE	6	2	305	Entry door
39	berth alongside	NE	7	2	305	Entry door
40	berth alongside	NE	7	2	305	Entry door

Note: When considering the limit berthing operation, the blowing wind has a great impact. The limit berthing condition of this experiment scheme is only the northeast wind, the falling flow rate is 3 knots, and the rising flow rate is 2 knots.

4. Statistics and Analysis of Simulation Test Results

This experiment utilized a large-scale ship maneuvering simulator to conduct berthing and unberthing maneuvering tests under various environmental conditions. The data recorded by the ship maneuvering simulator included heading, position, speed, angular velocity, main engine speed, water depth, wind direction, wind speed, current direction, and current speed at each sampling moment. The playback records can reproduce the simulation process, objectively reflecting the navigational trajectory of the simulated ship. By setting up ship maneuvering simulation tests under various navigation environments, the motion parameters and trajectories of the simulated ship were obtained. Combined with the potential risks of the maneuvering waters and berthing/unberthing operations, the safety of the navigational environment for the terminal engineering was assessed. This includes the analysis and evaluation of the safe turning waters and the safety of berthing/unberthing operations required for the safety assessment of the navigational environment of the terminal. This method is objective, feasible, and reasonable for the analysis and evaluation of the safety of berthing/unberthing operations at this terminal.

Although this project is a study on the ship maneuvering simulation for converting the Luojing operational area coal terminal to a container terminal, considering the overall planning of the Luojing operational area, this simulation not only included the berthing and unberthing maneuvers for the Phase I terminal but also simulated the berthing and unberthing maneuvers for the Phase II and Phase III terminals based on the overall engineering completion scenario.

Based on virtual simulation technology luojing container terminal scene model and luojing container terminal design ship model, carry out the design type in different wind, flow and narrow waters off the berthing operation simulation experiment, through simulation manipulation data statistical analysis and technical summary, ship berthing operation simulation test results as shown in figure 5 ~ figure 12.

A 10,000-ton container ship is berthing at the entrance gate with a speed of 10 kn and a heading of 133. NE wind level 6, flow rate 3 kn, flow to 125. Install two tugs to complete the berthing operation in berth 8. As shown in Figure 5.

A 10,000-ton container ship is berthing at the upstream water inlet gate, with a speed of 7.5 kn and a heading of 296. NE wind level 6, flow rate 3 kn, flow to 125. Install two tug to complete the berthing operation in berth 7. As shown in Figure 6.

A 10,000-ton container ship is berthing at the entrance gate, with a speed of 10 kn and a heading of 118. NE wind force 7, flow rate 3 kn, flow to 125. Install two tugs to complete the berthing operation in berth 8. As shown in Figure 7.

A 10,000-ton container ship is berthing at the upstream water inlet gate, with a speed of 7.5 kn and a heading of 296. NE wind force 7, flow rate 3 kn, flow to 125. Install two tugs to complete the berthing operation in berth 8. As shown in Figure 8.

A 10,000-ton container ship is berthing at the entrance gate, with a speed of 10 kn and a heading of 117. NE wind level 6, flow rate 2 kn, flow to 305. Install two tugs to complete the berthing operation in berth 8. As shown in Figure 9.

A 10,000-ton container ship is berthing at the upstream water inlet gate, with a speed of 7.6 kn and a heading of 295. NE wind level 6, flow rate 2 kn, flow to 305. Install two tug to complete the berthing operation in berth 7. As shown in Figure 10.

A 10,000-ton container ship is berthing at the entrance gate, with a speed of 10 kn and a heading of 123. NE wind force 7, flow rate 2 kn, flow to 305. Install two tugs to complete the berthing operation in berth 8. As shown in Figure 11.

A 10,000-ton container ship is berthing at the upstream water inlet gate, with a speed of 10 kn and a heading of 293. NE wind force 7, flow rate 2 kn, flow to 305. Install two tugs to complete the berthing operation in berth 8. As shown in Figure 12.

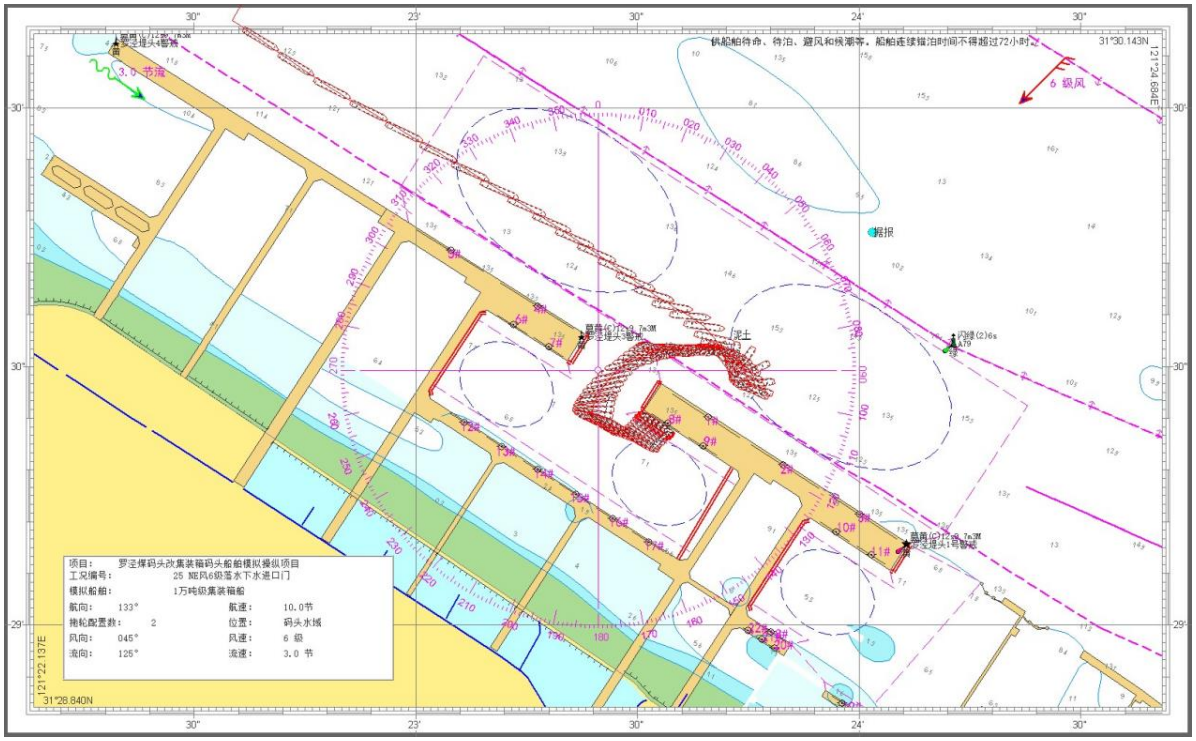

Figure 5. *Track diagram of the 10,000-ton container vessel (launching gate).*

Figure 6. *Track chart of 10000-ton container vessel (upper water inlet gate).*

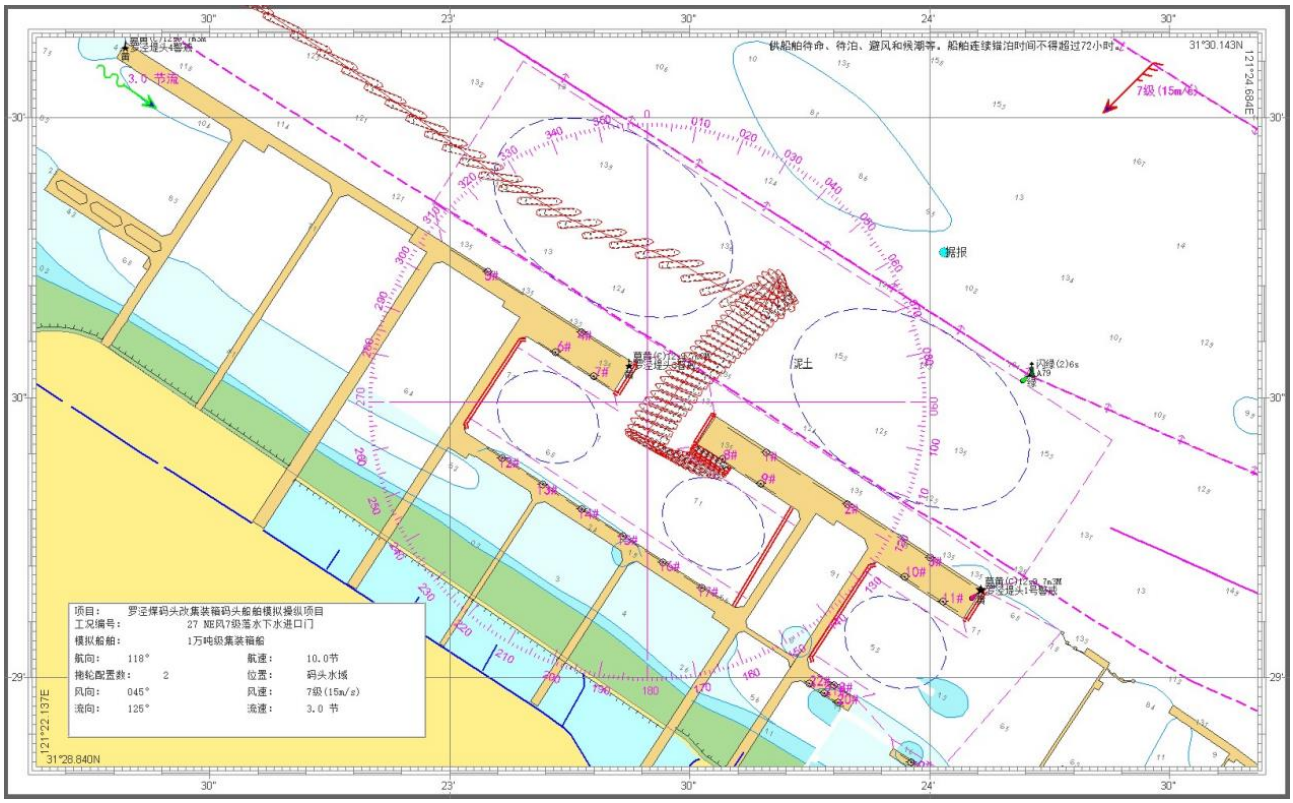

Figure 7. *Track diagram of 10,000-ton container ship NE 7 class (launching gate).*

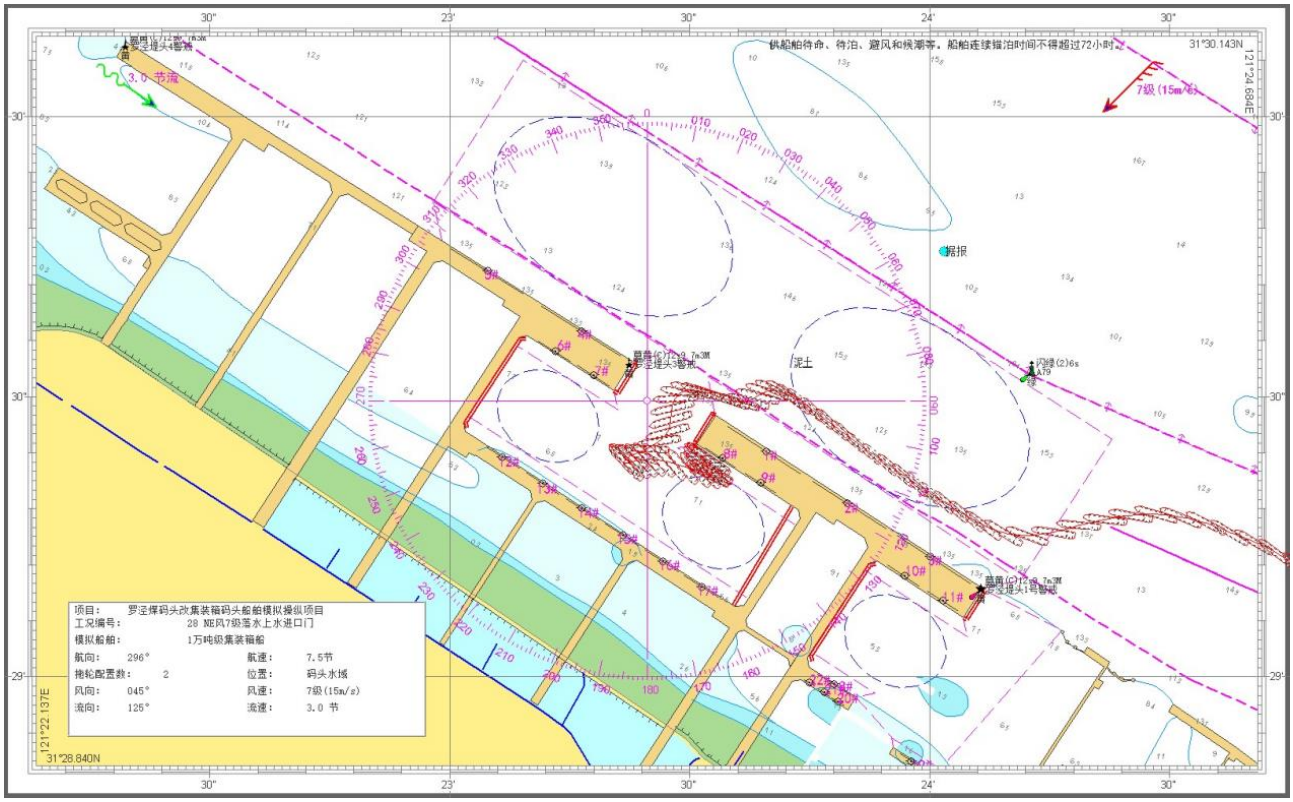

Figure 8. *Track chart of 10,000-ton container ship (upper water inlet gate).*

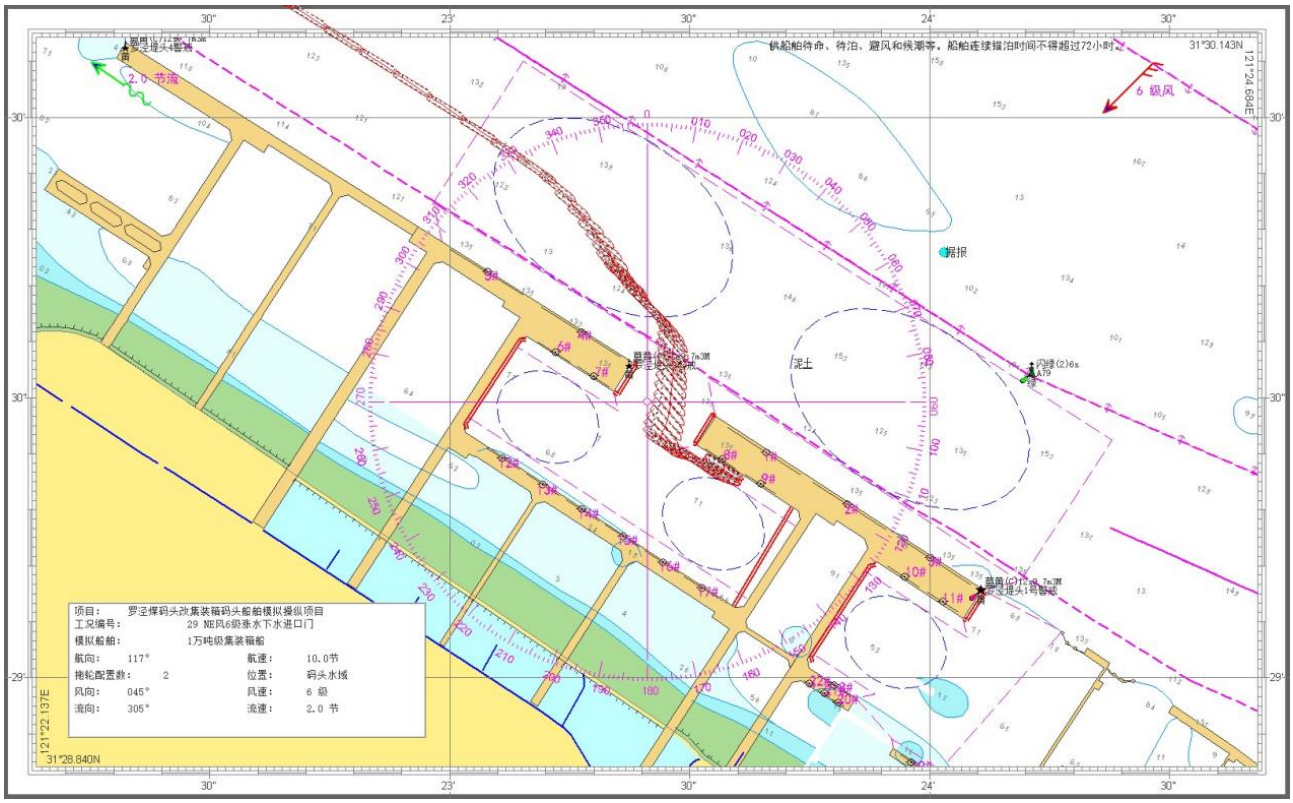

Figure 9. *Track diagram of the 10,000-ton container ship NE Class 6(inlet gate).*

Figure 10. *Track chart of 10,000-ton container ship (upper water inlet gate).*

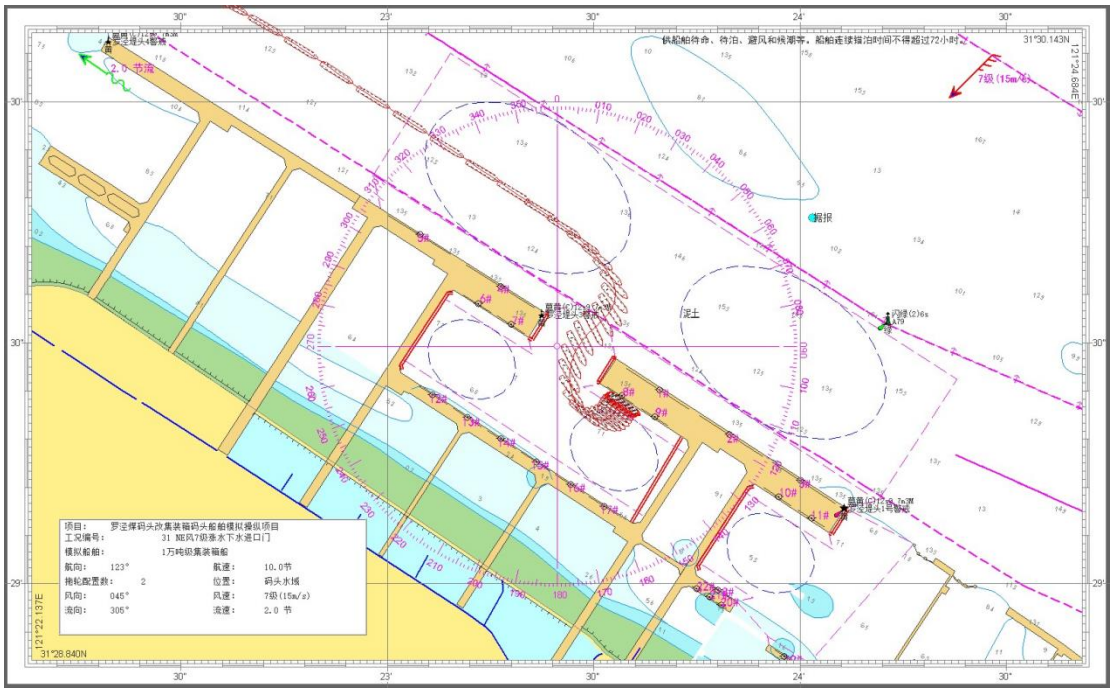

Figure 11. *Track chart of 10,000-ton container ship NE wind class 7 high tide (water inlet gate).*

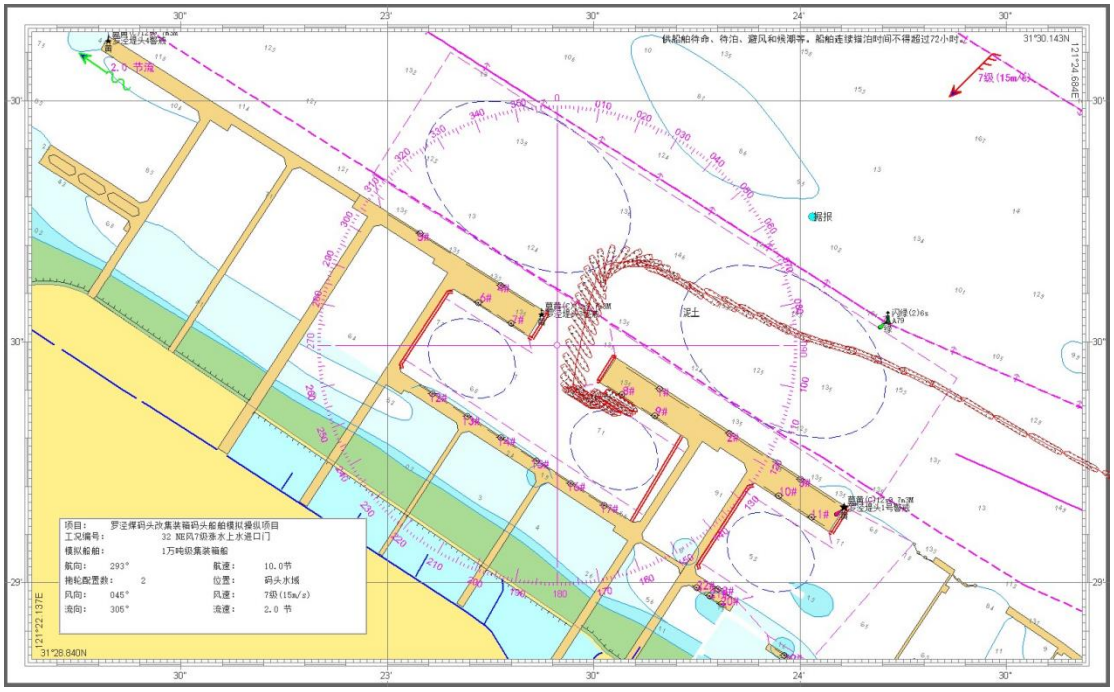

Figure 12. *Track chart of 10,000-ton container ship (upper water inlet gate).*

5. Conclusion

By analyzing the ship berthing simulation trajectory diagrams under the above eight extreme berthing conditions, the use of tugs, and the usage of ship's engine and rudder, the following conclusions can be drawn:

Due to the relatively large power of the two assisting tugs compared to a 10,000-ton container ship, the impact of wind force on the berthing of the 10,000-ton container ship is minimal. The ship can complete berthing operations under wind force of levels 6 or 7, regardless of whether it is during rising or falling tide, with the assistance of two tugs with 3000 kW power each.

Considering that after the reconstruction, the flow in the engineering waters will be almost perpendicular to the en-

trance of the small terminal harbor basin channel, with a maximum intersection angle of 87.6 °, the ship will be significantly affected by the current when entering or exiting the channel, and the entrance width is only 300 meters. When the wind force reaches level 8 or above, pilots can decide whether to proceed with the berthing operation based on the actual environmental and ship conditions at that time.

Based on the ship maneuvering simulation tests, berthing operations under extreme sea conditions can be carried out at any time except during the peak regulation periods specified by maritime authorities. Additionally, it is safer to choose berthing during periods when the current is relatively weak.

Before conducting berthing operations under extreme sea conditions, full consideration should be given to the impact of extreme conditions on the ship and the visual impact of berthed ships at the entrance. Ships must use AIS information and communicate their dynamics to detect and avoid potential traffic in the Baoshan South Channel in advance. Coordination and avoidance should be timely, and the peak traffic periods in the Baoshan South Channel should be avoided for safe passage through the entrance.

Under extreme sea conditions, before a 10,000-ton container ship berths at the small terminal, tugs should be positioned as early as possible. For feeder ships berthing independently, it is necessary to adjust the ship's position in advance based on actual conditions and control the ship's speed entering the entrance at a favorable small angle against the current to suit the prevailing wind and current conditions.

When berthing under extreme sea conditions, significant wind and current pressure differences can occur. To ensure sufficient maneuverability, pilots should fully consider the impact of wind and current, maintain an appropriate ship speed, control the ship's residual speed, and adjust the berthing angle and lateral distance (maintaining a lateral distance of no less than four times the ship's width under strong crosswind conditions and around two times the ship's width under strong headwind conditions), and operate with extreme caution.

When conducting berthing operations under extreme sea conditions, the impact of tides should be fully considered, avoiding berthing during rapid rising or falling tides. The visual impact of the terminal and berthed ships should also be fully considered. Furthermore, berth information should be confirmed in advance to avoid situations where the berth is not clear upon arrival, requiring waiting or anchoring. It is also recommended that the authorities establish an emergency anchorage area at the Baoshan South Anchorage.

Abbreviations

MMG	Mathematical Maneuvering Group
VTI	Vertical Transverse Isotropy
NSCD	Nested Random Composite Distribution
LNG	Liquefied Natural Gas

Author Contributions

Haidong Zhan: Writing – original draft, Writing – review & editing

Feng Zhu: Data curation, Methodology

Jianwen Wu: Formal Analysis, Validation

Jie Wang: Resources, Supervision

Conflicts of Interest

The authors declare no conflicts of interest.

References

[1] Zhang Yecheng, Zhan Chengcheng and Shang Haodong. (2023). Numerical simulation of the motion based on four degrees of freedom. Journal of Wuhan University of Technology (Transportation Science and Engineering Edition) (04), 659-664.

[2] Wu Rocinante, Lu Yun. A hydrodynamic coefficient measurement method based on the Stewart six-degrees of freedom ship constraint model test platform [J]. Journal of Wuhan University of Technology (Transportation Science and Engineering Edition), 2023, 47(03): 465-471.

[3] Yi Cong, Yu Boqian, Lu Wenyue, etc. Effect of wave flow coupling on the motion response of cylindrical type FPSO [J]. China Marine Platform, 2023, 38(05): 42-48 + 59.

[4] Erik V. Analyzing Extreme Sea State Conditions by Time-Series Simulation Accounting for Seasonality [J]. J. Offshore Mech. Arct. Eng, 2023, 145(5).

[5] Mingxin L, Suyong P, Yong C, et al. Time-domain numerical simulation for multi-ships moving in waves with forward speed [J]. Ocean Engineering, 2023, 290.

[6] Mingyu Y, Zhenjun Z, Zhongbin S, et al. Numerical evaluation of the tension mooring effects on the hydrodynamic response of moored ships under harbor oscillations [J]. Ocean Engineering, 2023, 288(P2).

[7] Hongwei H, Thibaut Z V, Evert L, et al. Model predictive controller for path following ships validated by experimental model tests [J]. Ocean Engineering, 2023, 288(P2).

[8] Bingjie G, Prateek G, Sverre S, et al. Evaluating vessel technical performance index using physics-based and data-driven approach [J]. Ocean Engineering, 2023, 286(P2).

[9] Gabriel J B R, Andrés G, Cabello J J E. Vortex-induced vibration effect of extreme sea states over the structural dynamics of a scaled monopile offshore wind turbine [J]. Journal of Ocean Engineering and Marine Energy, 2022, 9(2): 359-376.

[10] Guilin L, Xinsheng Z, Yi K, et al. Analysis of extreme sea states under the impact of typhoon in different periods: A nested stochastic compound distribution applied in the South China Sea [J]. Applied Ocean Research, 2022, 127.

[11] Huang Ming, Dou Peijun, Wang Yuping, etc. Analysis of unberthing operation of LNG ships in bad weather based on virtual simulation and real ship verification [J]. Journal of Wuhan University of Technology (Transportation Science and Engineering edition), 2022, 46(04): 743-748.

[12] Meng Yao. Mathematical model of ship manipulation motion based on grey Wolf-support vector machine identification [D]. Dalian Maritime University, 2022. https://doi.org/10.26989/d.cnki.gdlhu.2022.000989

[13] Bian Hongwei, Zhu Zhonglei, Wang Rongying, etc. A vessel motion parameter generator based on an A & ω six-degrees of freedom motion model [J]. Systems Engineering and Electronics Technology, 2022, 44(08): 2628-2634.

[14] Zhang Yue. Simulation and application of pitch paddle device in ship side push system [D]. Maritime Affairs University of Dalian, 2022. https://doi.org/10.26989/d.cnki.gdlhu.2022.001474

[15] Qianfeng J, Kenji S, Chen C, et al. Analysis of ship maneuvering difficulties under severe weather based on onboard measurements and realistic simulation of ocean environment [J]. Ocean Engineering, 2021, 221.